Electronic Supplementary Material (ESI) for Nanoscale.
This journal is © The Royal Society of Chemistry 2024

Electronic supplementary information

2-mercaptobenzothiazole and 2-mercaptobenzimidazole derived novel Ag_{16} and Ag_{18} nanoclusters: Synthesis and optical properties

BedantaBorah[a], Rohan Sharma[a], Pankaz K. Sharma[a]* and Apurba Kr. Barman[a]*

Department of Chemistry, Cotton University, Panbazar, Guwahati, Assam, INDIA,781001

Table of contents

Experimental section:

Instrumentation: The FTIR spectra of Ag-MBTNC and Ag-MBINC was recorded in a Bruker APEX II spectrophotometer in the frequency range 500-4000 cm^{-1} (KBR phase). UV-visible absorption spectrum of Ag-MBTNC and Ag-MBINC were measured up through Shimadzu UV-2600 spectrophotometer (model no. UV-18000). In these measurements the two nanoclusters are dissolved in ethanol under sonication and in these measurements the spectrum are recorded from 200 nm to 1400 nm range in quartz cuvette having 1cm optical path length. The photoluminescence spectrum of two nanoclusterswere recorded in Horiba FluoroMax-4 instrument by exciting the nanoclusters from 264 to 270 nm range. Photoluminescence decay lifetime measurements were carried out on a time-correlated single photon counting (Edinburgh Instruments-Lifespec II) using a pulsed laser at 375 nm with an fwhm of ~153 ns. The MALDI-TOF mass spectrometry were conducted by using Bruker, Model: Autoflex speed mass spectrometer in appositive mode by using sinapic acid as a matrix at (at 1:100 ratio of sample to matrix). For MALDI MS studies a pulsed nitrogen laser of 337 nm was used. The X-ray photoelectron spectroscopy (XPS) was used to evaluate the chemical composition of nanoclusters by using a Thermo-Scientific ESCALAB Xi^{+} (UK) with a monochromatic Al Kα X-ray source (1486.6 eV). RigakuUltimaIV X-ray powder diffractometer was used for PXRD measurements of all the nanoclusters with a Cu Kα X-ray source, equipped with a Ni filter to suppress Kβ emission and a D/teXUltra high-speed position sensitive detector, and measurements were performed at room temperature, with a scan rate of 10º min^{-1}, scan range 2θ= 5-50º, and step size of 0.02º.Thermogravimetric (TG) measurements of two nanoclusters were performed on a Mettler Toledo instrument with a temperature range of 25-700 ºC and a heating rate of 20 ºC min^{-1}. Nanoclusters were placed in silica crucibles and purged by a steam of nitrogen flowing at 80 mL

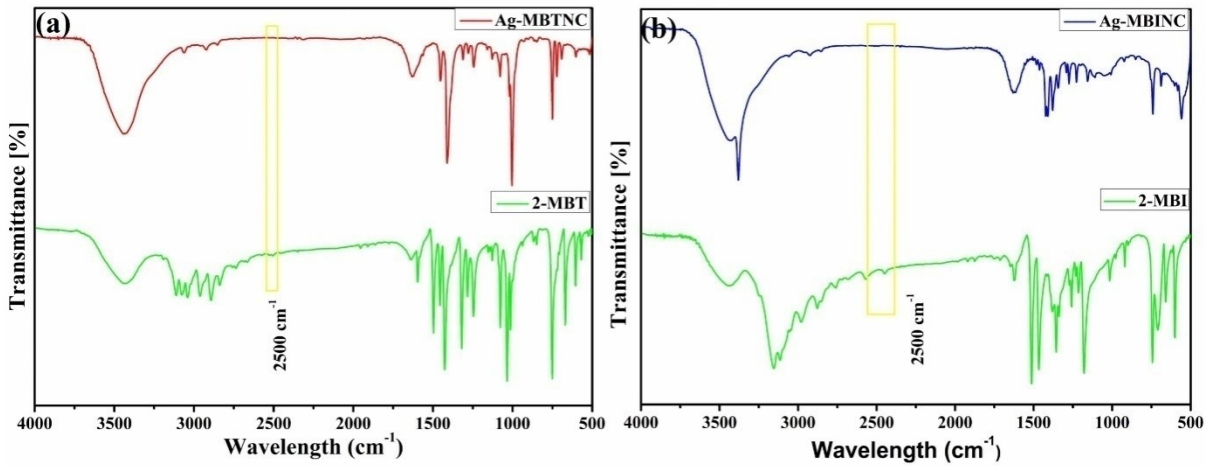

Figure S1. FTIR spectra of (a) 2-MBT (green) and Ag-MBTNC (red), (b) 2-MBI (green) and Ag-MBINC (blue).

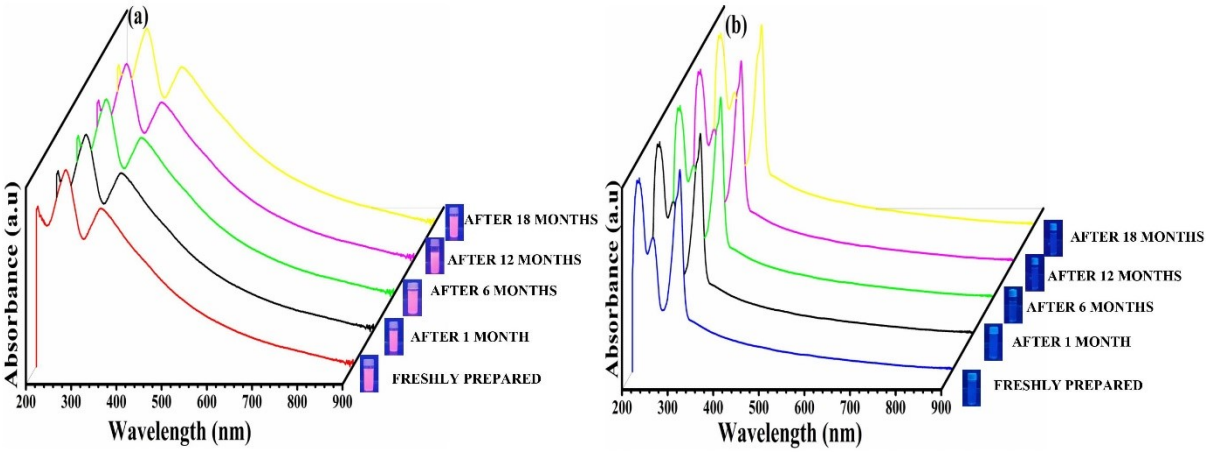

Figure S2. UV-visible spectra of (a) Ag-MBTNC in ethanol: freshly prepared, after one month, after 6 months, after 12 months and after 18 months (b) Ag-MBINC in ethanol: freshly prepared, after one month, after 6 months, after 12 months and after 18 months.

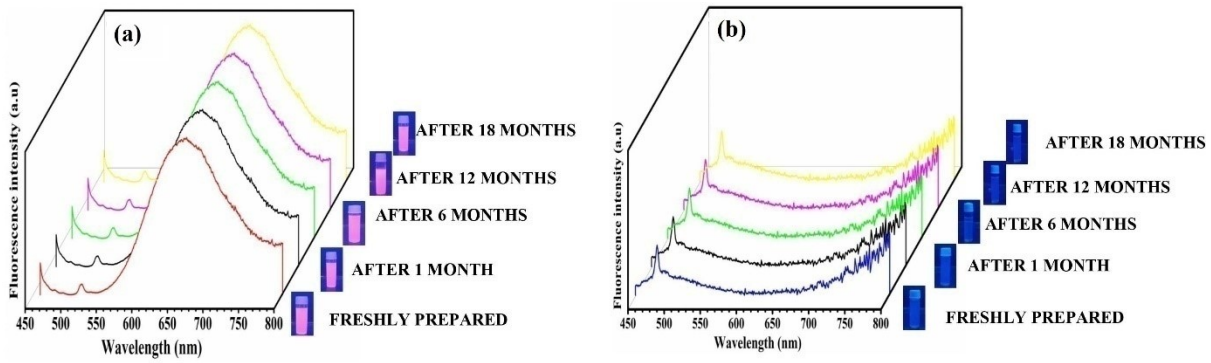

Figure S3. Photoluminescence spectrum of (a) Ag-MBTNC (in aqueous ethanol): freshly prepared, and freshly prepared solution of one month, 6 months, 12 months and 18 months old nanoclusters(b) Ag-MBINC (in aqueous ethanol): freshly prepared, and freshly prepared solution of one month, 6 months, 12 months and 18 months old nanoclusters.

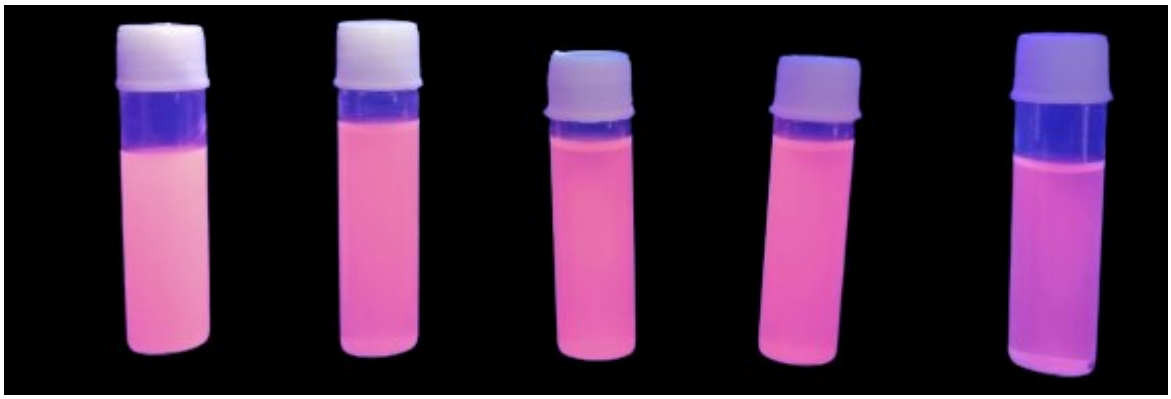

(I) (II) (III) (IV) (V)

Figure S4. Photographs of ethanolic solution of Ag-MBTNC under UV light: freshly prepared (I)and freshly prepared solution of one month (II), 6 months (III), 12 months (IV) and 18 months (V)old nanoclusters.

Quantum yield (QY) calculation:

The QY of Ag-MBTNC (sample) was determined from the slope of plot (Absorbance vs. maximum emission intensity). Here, quinine sulphate (in 0.1 M H_2SO_4) was taken as standard with a known QY of 54%. Ag-MBTNC was dissolved in ethanol. The following equation is used for QY measurement.

$$QY_{sample} = QY_{std} \times \left(\frac{K_{sample}}{K_{std}}\right) \times \left(\frac{\eta_{sample}}{\eta_{std}}\right)^2$$

where K is the slope determined from the graph, and η is the refractive index of the solvent (refractive index of ethanol is 1.36). The same excitation wavelength (350 nm) and band width were applied to the sample and the standard.

Slope (sample)	Slope (standard)	$\left(\eta_{sample}/\eta_{std}\right)^2$	QY_{std}	QY_{sample}
1.15×10^6	6.90×10^6	1.85	54%	16.65%

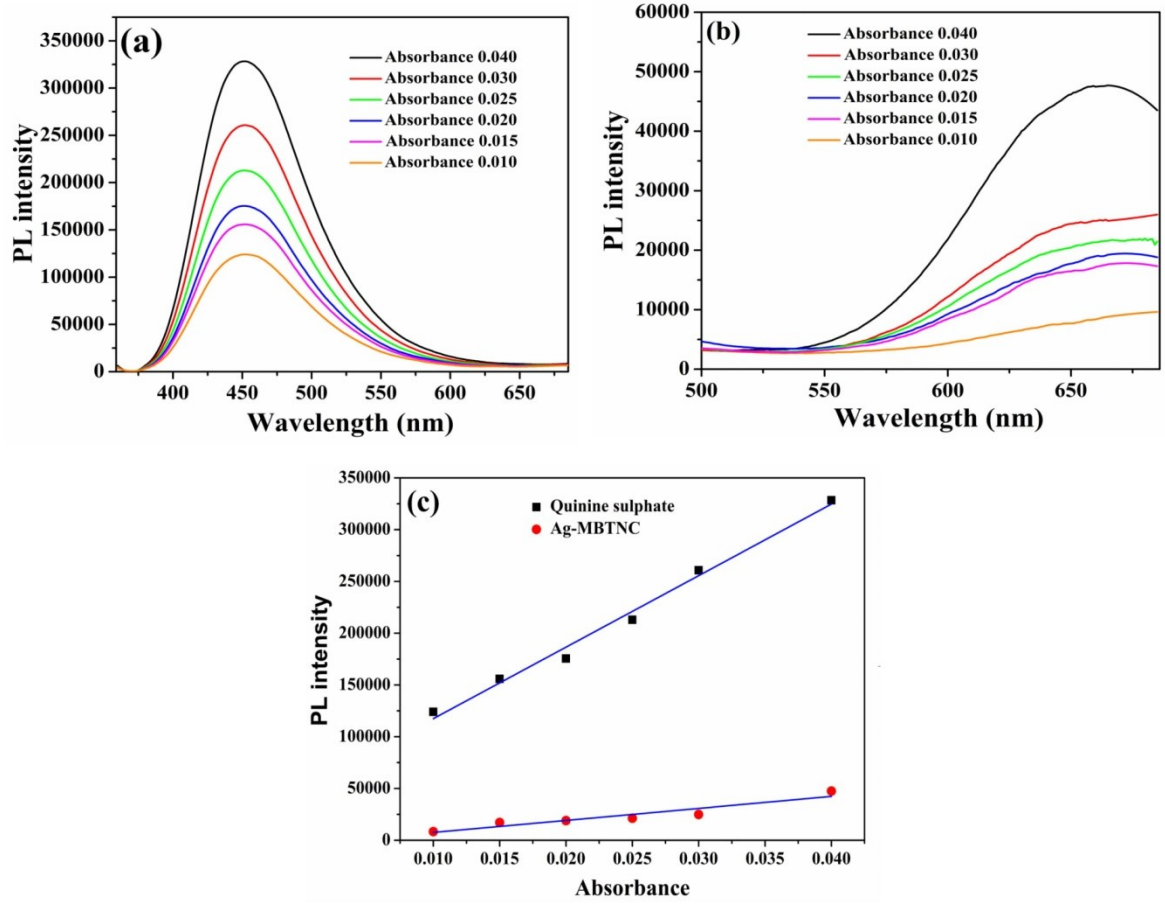

Figure S5: Comparative photoluminescence spectra for (a) quinine sulphate (b) Ag-MBTNC at the same excitation wavelength and with the same absorbance at excitation wavelength. (c) Plot of maximum emission intensity vs absorbance used for QY calculations.

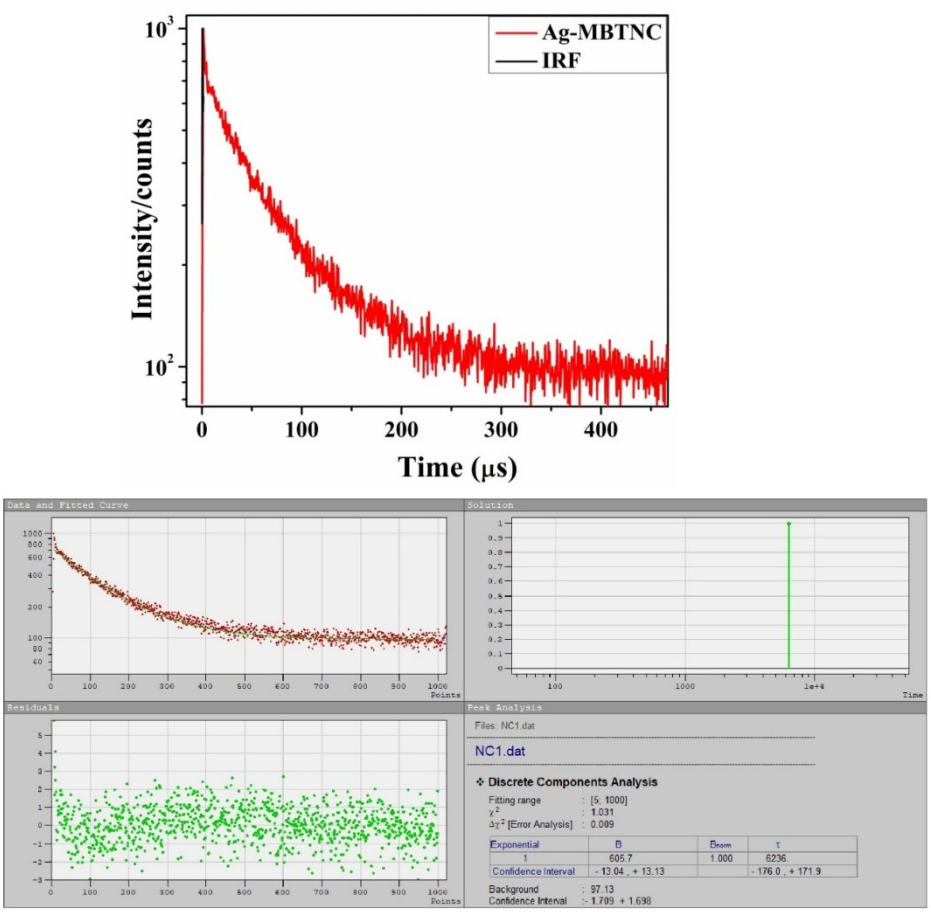

Figure S6: Fluorescence life time decay of Ag-MBTNC.

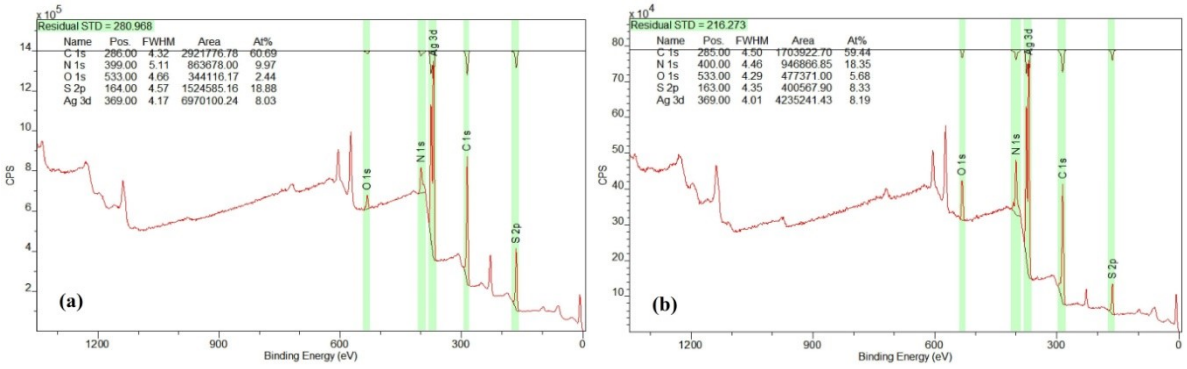

Figure S7. Atomic percentages from XPS spectra of (a) Ag-MBTNC and (b) Ag-MBINC.

Table T1. Relative atomic percentages of C, S, N, O and Ag with respect to S in Ag-MBTNC.

NAME OF THE ELEMENTS	ATOMIC PERCENTAGE (%) from XPS data	RATIO	
		EXPERIMENTAL	THEORITICAL
CARBON (C)	~60.69	C/S=3.21	89 C/24 S=3.70
SULPHUR (S)	~18.88	S/S=1	24 S/24 S=1
NITROGEN (N)	~9.97	N/S=0.52	12 N/24 S=0.55
OXYGEN (O)	~2.44	O/S=0.12	4 O/24 S=0.16
SILVER (Ag)	~8.03	Ag/S=0.42	16 Ag/24 S=0.66

Table T2. Relative atomic percentages of C, S, N, O and Ag with respect to S in Ag-MBINC.

NAME OF ELEMENTS	ATOMIC PERCENTAGE (%)	RATIO	
		EXPERIMENTAL	THEORITICAL
CARBON (C)	~59.44	C/S=7.13	88 C/12 S=7.33
SULPHUR (S)	~8.33	S/S=1	12 S/12 S=1
NITROGEN (N)	~18.35	N/S=2.20	24 N/12 S=2
OXYGEN (O)	~5.68	O/S=0.68	4 O/12 S=0.33
SILVER (Ag)	~8.19	Ag/S=0.98	18 Ag/12 S=1.50

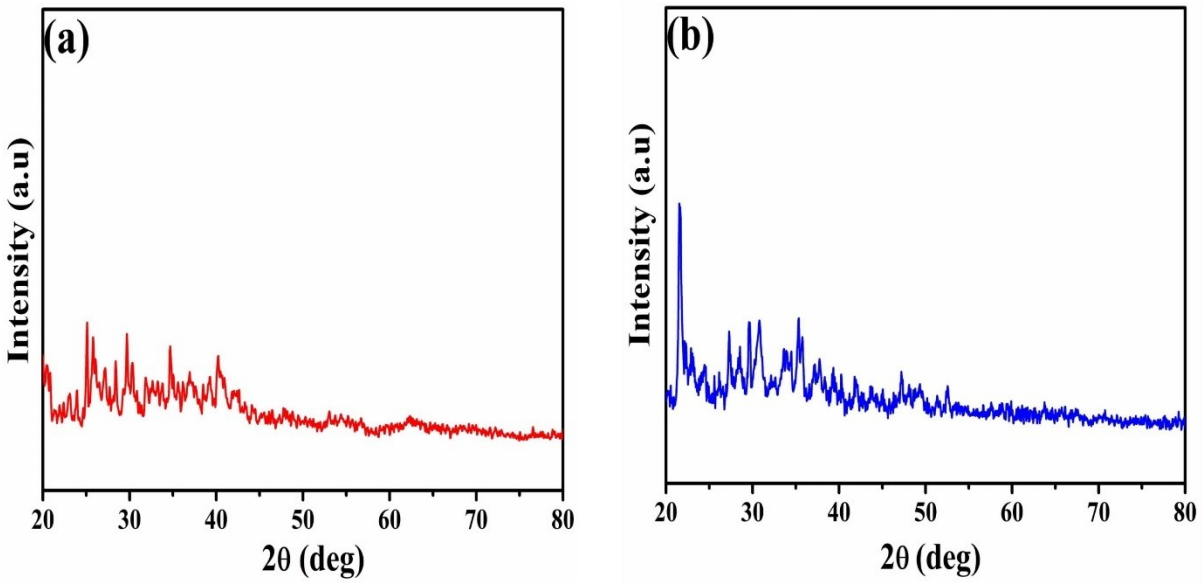

Figure S8. PXRD patterns of (a) Ag-MBTNC and (b) Ag-MBINC

Table T3. TGA data of Ag-MBTNC

Name	Molecular weight	Experimental	Theoritical
Ag-MBTNC ($C_{89}H_{66}Ag_{16}N_{12}O_4S_{24}$)	3863.0		
Solvent ($C_5H_{18}O_4$)	142.2	3.6%	3.7%
Ligand ($C_{84}H_{48}N_{12}S_{24}$)	1994.9	52.2%	51.6%
Silver residue (Ag_{16})	1725.8	44.2%	44.7%

Table T4.TGA data of Ag-MBINC

Name	Molecular weight	Experimental	Theoritical
Ag-MBINC ($C_{88}H_{76}Ag_{18}N_{24}O_4S_{12}$)	3860.1		
Solvent ($C_4H_{16}O_4$)	128.1	4.0%	3.3%
Ligand ($C_{84}H_{60}N_{24}S_{12}$)	1790.3	46.6%	46.4%
Silver residue (Ag_{18})	1941.6	49.4%	50.3%

Computational Details

All the structures were optimized using the PBE0[1] functional and the Def2-TZVP basis sets with ORCA 5.0.3.Grimme's third-order dispersion correction was incorporated with Becke-Johnson dumping to properly take into account the effect of dispersion in our studied systems. The Effect of the solvent, methanol, was gauzed with the implicit polarizable continuum model CPCM with ORCA 5.0.3.The NBO calculations were carried out using the above mentioned model chemistry to obtain the HOMO and the LUMO energy values and their energy gap. Moreover, NICS calculations were performed at the PBE0/Def2-TZVP level of theory, to investigate the aromatic nature of the molecules before and after incorporating the Ag^{+} metal ion. Both the NBO and NICS calculation were performed in Gaussian16.

Computational results:

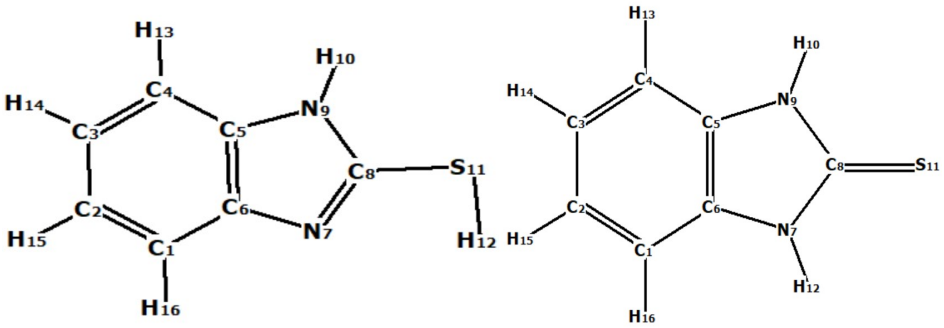

2-MBI thione form (1a) **2-MBI thiol form (1b)**

Table T5: Selected structural parameters of tautomers**2-MBI**.The distances are given in Å.

Parameter	2-MBI thione form (1a)	2-MBI thiol form (1b)
C1-C2	1.39	1.38
C1-C6	1.38	1.39
C2-C3	1.39	1.40
C5-C6	1.40	1.41
C6-N7	1.38	1.38
N7-C8	1.37	1.30
N7-H12	1.00	----
C8-C9	1.37	1.37
C8-S11	1.65	1.74
N9-H10	1.00	1.00
S11-H12	----	1.34

The energy difference between **1a** and **1b** is 12.90 Kcal mol^{-1} i.e., **1a** is 12.90 Kcal mol^{-1} more stable than that of **1b**.

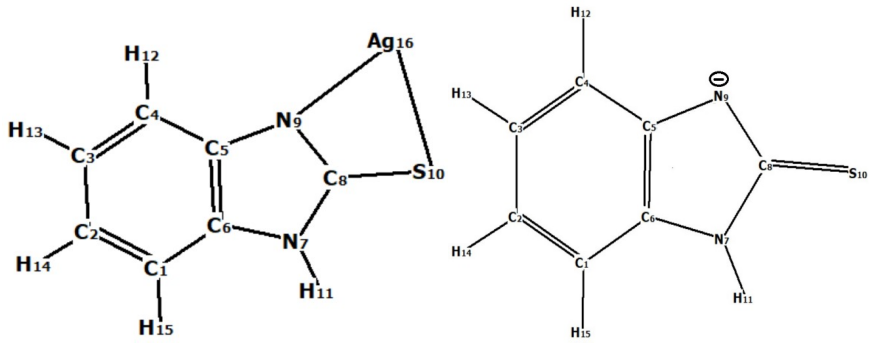

1a (-) _Ag^+ **1a (-)**

This is the structure obtained upon addition of Ag^+ to the 1a (-).

Table T6: Selected structural parameters of **1a (-) -Ag(I)**.The distances are given in Å.

	N9-Ag16	S10-Ag16	N9-C8	C8-S10
1a (-) _Ag^+	2.36	2.48	1.33	1.72

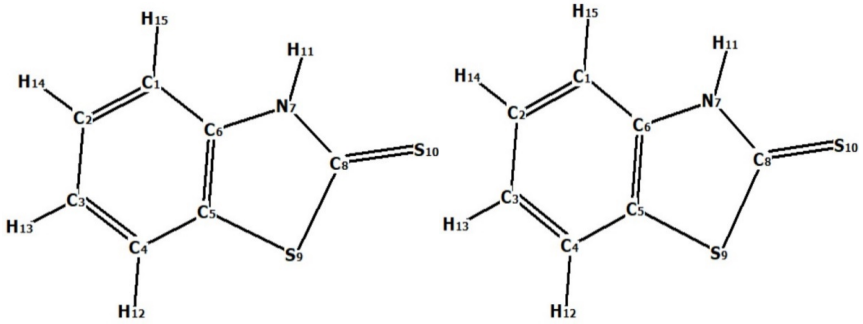

2-MBT thione form (2a) **2-MBT thiol form (2b)**

Table T7: Selected structural parameters of**2a** and **2b**. The distances are given in Å.

Parameter	**2a**	**2b**
C1-C2	1.38	1.38
C1-C6	1.39	1.39
C2-C3	1.39	1.40
C5-C6	1.40	1.41
C5-S9	1.74	1.73
C6-N7	1.38	1.38
N7-C8	1.36	1.29
N7-H11	1.01	----
C8-S9	1.75	1.75
C6-S10	1.64	1.74

The energy difference between **2a** and **2b is** 8.16 Kcal mol^{-1} i.e., **2a** is 8.16 Kcal mol^{-1} more stable than that of **2b**.

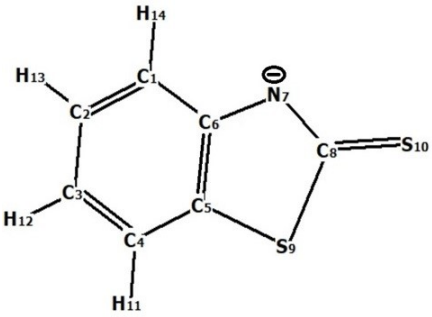

2a(-)

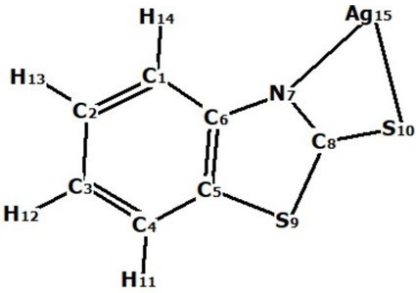

2a_1 (-) _Ag^+

This structure is obtained upon addition of Ag^+ to the 2a_1 (-).

Table T8: Selected structural parameters of**2a_1 (-) _Ag^+**.The distances are given in Å.

	N7-Ag15	S10-Ag15	N7-C8	C8-S10
2a_1 (-) _Ag^+	2.42	2.45	1.31	1.71

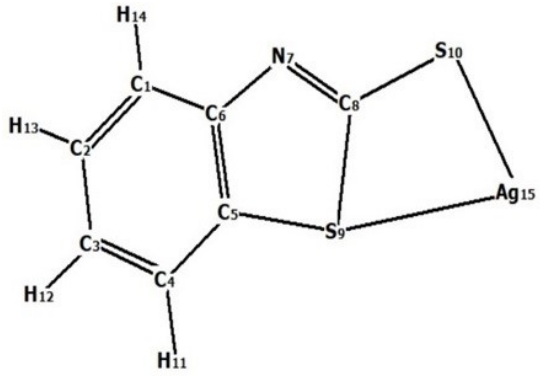

2a_2 (-) _Ag^+

This structure is obtained upon addition of Ag^+ to the **2a_2 (-).**

Table T9: Selected structural parameters of**2a_2 (-) _Ag^+**.The distances are given in Å.

	S9-Ag15	S10-Ag15	N7-C8	C8-S10
2a_2 (-) _Ag^+	3.21	2.34	1.29	1.73

From the above data, it is evident that the **2a_1 (-) _Ag$^+$** is 6.93 kcal mol^{-1} more stable than **2a_2 (-) _Ag$^+$.** This indicates that the addition of Ag$^+$ to the **2a(-)**molecule favors the addition from N and S as coordinating atoms rather than S and S.

In Methanol (ε= 32.63**)**

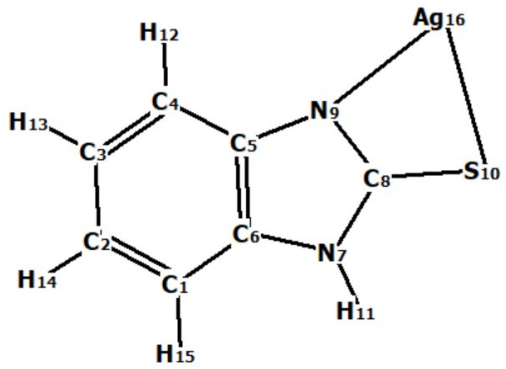

1a (-)_Ag$^+$(in methanol)

Table T10: Selected structural parameters of **1a_(-) _Ag$^+$** in methanol. The distances are given in Å.

=	N9-Ag16	S10-Ag16	N9-C8	C8-S10
1a (-) _Ag$^+$	2.49	2.47	1.33	1.72

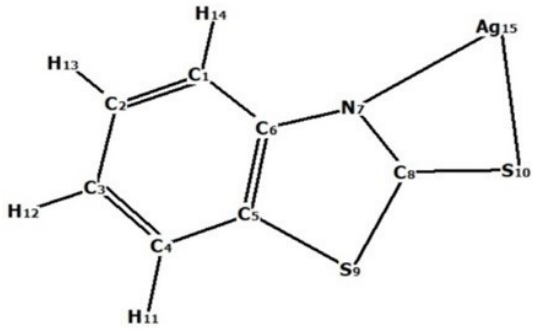

2a_1 (-)_Ag$^+$(in methanol)

Table T11: Selected structural parameters of **2a_1(-)_Ag$^+$** in methanol. The distances are given in Å.

	N7-Ag15	S10-Ag15	N7-C8	C8-S10
2a_1 (-)_Ag$^+$	2.72	2.42	1.30	1.72

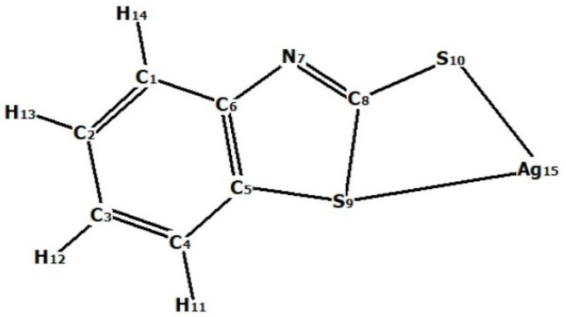

2a_2 (-) _Ag$^+$(Methanol)

Table T12: Selected structural parameters of **2a_2(-)_Ag$^+$** in methanol. The distances are given in Å.

	S9-Ag15	S10-Ag15	N7-C8	C8-S10
2a_2 (-) _Ag$^+$	3.31	2.36	1.30	1.73

From the above data, it is evident that **2a_1 (-)_Ag$^+$** is1.56 kcal mol-1 more stable than **2a_2 (-) _Ag$^+$** in methanol.

NICS computation: The NICS method is used to evaluate the aromatic nature of the molecules. The NICS (0), NICS (0.5), NICS (1) and NICS $(1)_{ZZ}$ are calculated though the NICS (1) and NICS $(1)_{ZZ}$ are more reliable for the study of aromaticity. For the purpose of comparison, the NICS values of benzene are also calculated. The more negative the NICS value, the more pronounced is the aromatic character of the molecule.

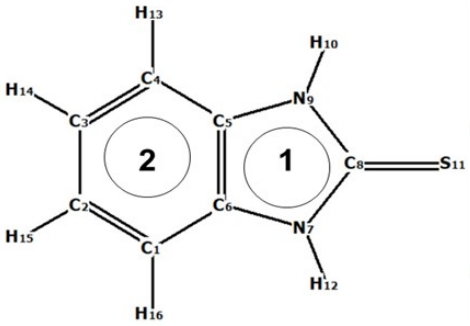

1a

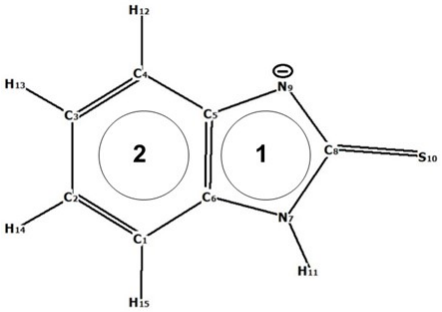

1a (-)

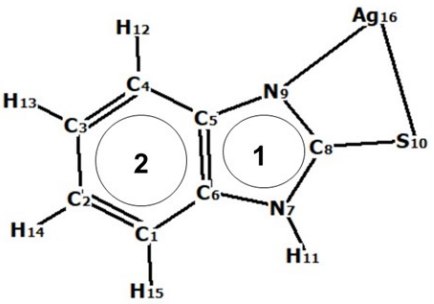

1a(-)_Ag$^+$

Table T13: NICS Values (ppm) for compound 1a, 1a(-) and 1a(-)_Ag$^+$

Molecules	On ring 1				On ring 2			
	NICS (0)	**NICS (0.5)**	**NICS (1)**	**NICS $(1)_{ZZ}$**	**NICS (0)**	**NICS (0.5)**	**NICS (1)**	**NICS $(1)_{ZZ}$**
1a	-7.3	-7.4	5.4	-14.0	-9.7	-10.8	10.0	-27.9
1a(-)_Ag$^+$	-8.8	-9.6	-7.6	-20.0	-10.1	-11.2	-10.4	-29.1

The NICS values of benzene using the same model chemistry are

NICS (0) = -8.2 ppm

NICS (0.5) =-10.0 ppm

NICS (1) = -10.1 ppm

NICS $(1)_{ZZ}$ = -30.2 ppm

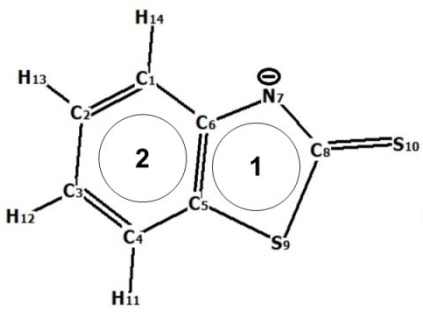

2a (-)

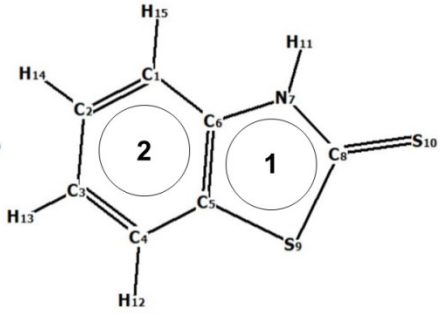

2a

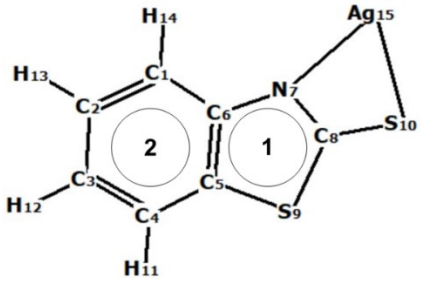

2a_1 (-) _Ag^+

Table T14: NICS Values (ppm) for compounds 2a, 2a(-) , 2a_1(-)_Ag^+ and 2a_2(-)_Ag^+

Molecules	On ring 1				On ring 2			
	NICS (0)	NICS (0.5)	NICS (1)	NICS $(1)_{ZZ}$	NICS (0)	NICS (0.5)	NICS (1)	NICS $(1)_{ZZ}$
2a	-5.8	-5.6	-4.0	-8.6	-8.7	-10.0	-9.5	-27.0
2a_1(-)_Ag^+	-7.0	-7.7	-6.5	-14.6	-9.2	-10.6	-10.0	-28.1

Table T15: The HOMO and the LUMO energies (a.u.) and the HOMO-LUMO energy gap (eV) of compounds 1a, 1a(-) and 1a(-)_Ag^+

Molecule	E_{HOMO}(au)	E_{LUMO}(au)	$\|\Delta E_{H-L}\|$(eV)
1a	-0.21642	-0.03437	4.95
1a(-)	-0.03782	0.12552	4.44
1a(-)_Ag^+	-0.20762	-0.08870	3.24

Table T16: The HOMO and the LUMO energies (a.u.) and the HOMO-LUMO energy gap (eV) of compounds2a, 2a(-) , 2a_1(-)_Ag^+ and 2a_2(-)_Ag^+

Molecule	E_{HOMO}(au)	E_{LUMO}(au)	$\|\Delta E_{H-L}\|$(eV)
2a	-0.22739	-0.04890	4.86
2a(-)	-0.04901	0.11422	4.44
2a_1(-)_Ag^+	-0.21723	-0.09518	3.32

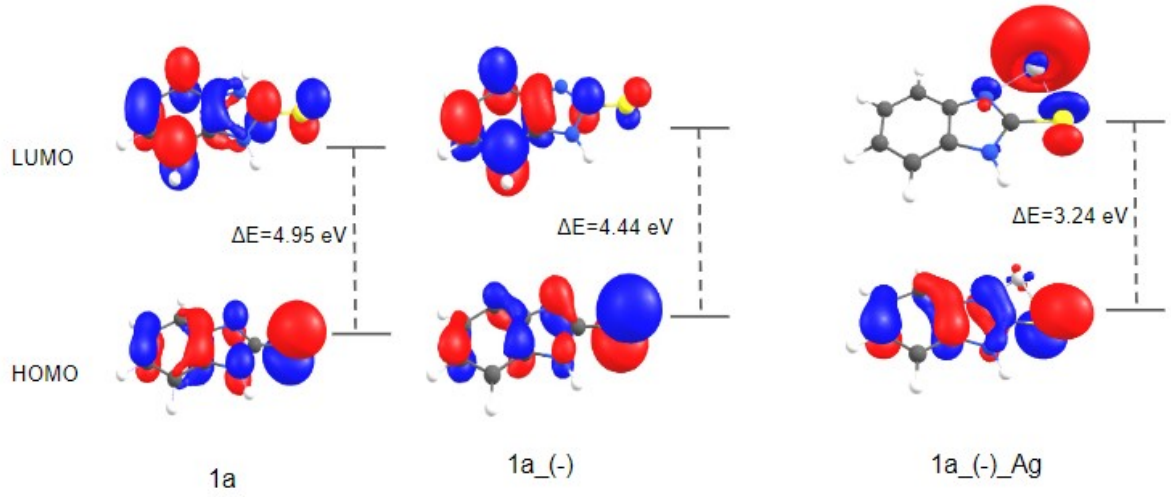

Figure S9. The HOMO, the LUMO and their energy gap of **1a** derivatives.

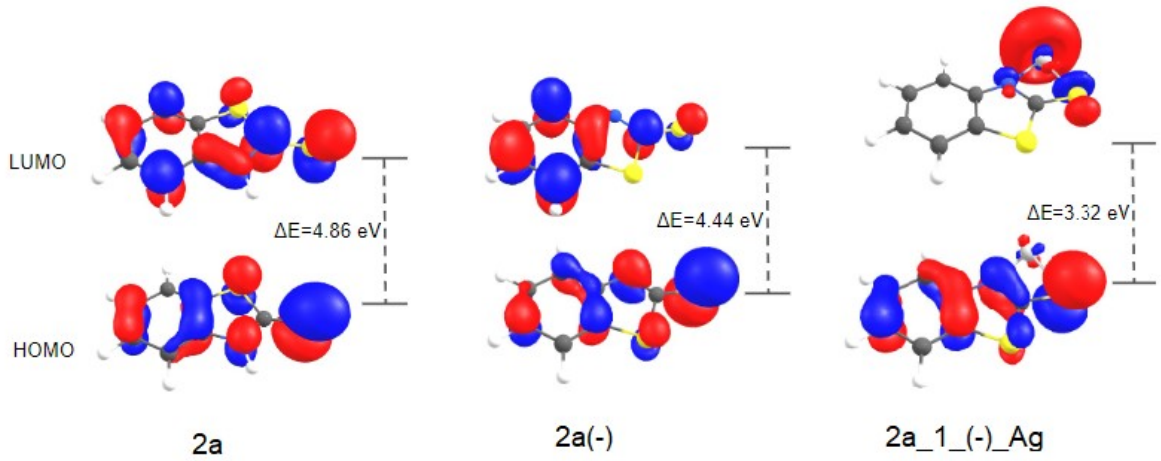

Figure S10. The HOMO, the LUMO and their energy gap of the **2a** derivatives.

Table 17: Selected bond lengths for interaction of 2-MBT with both Ag (I) and Ag (0). (Fig 9a main text)

Parameter	Values (Å)
S1-Ag10	3.31
S8-Ag10	2.50
S8-Ag9	2.54
N3-Ag9	2.45

Table 18: Selected bond lengths for interaction of 2-MBI with both Ag (I) and Ag (0). (Fig 9b main text)

Parameter	Values (Å)
N1-Ag10	3.37
S8-Ag10	2.51
S8-Ag9	2.58
N3-Ag9	2.33

The co-ordinates of the optimized structures reported in this manuscript

The optimizations were done using the PBE0 density functional with the incorporation of Grimme's third-order dispersion correction with Becke-Johnson dumping. The Def2-TZVP basis sets were used in the calculations.

1a

Atom	X	Y	Z
6	1.419411000	0.000000000	1.807792000
6	0.695698000	0.000000000	2.994703000
6	-0.695698000	0.000000000	2.994703000
6	-1.419411000	0.000000000	1.807792000
6	-0.700862000	0.000000000	0.627924000
6	0.700862000	0.000000000	0.627924000
7	1.081444000	0.000000000	-0.697058000
6	0.000000000	0.000000000	-1.532478000
7	-1.081444000	0.000000000	-0.697058000
1	-2.017534000	0.000000000	-1.061093000
16	0.000000000	0.000001000	-3.179766000
1	2.017533000	0.000000000	-1.061093000
1	-2.502496000	0.000000000	1.809877000
1	-1.227846000	0.000001000	3.937975000
1	1.227846000	0.000001000	3.937975000
1	2.502496000	0.000000000	1.809877000

1a (-)

Atom	X	Y	Z
6	1.802516000	1.412037000	0.000000000
6	2.993098000	0.684554000	0.000000000
6	2.976647000	-0.709323000	0.000000000
6	1.781283000	-1.421682000	0.000000000
6	0.577449000	-0.720664000	0.000000000
6	0.616746000	0.700103000	0.000000000
7	-0.698434000	1.058778000	0.000000000
6	-1.490457000	-0.089125000	0.000000000
7	-0.709851000	-1.172218000	-0.000001000
16	-3.177688000	0.042718000	0.000001000
1	-1.098852000	1.978196000	0.000000000
1	1.773083000	-2.506353000	0.000000000
1	3.918383000	-1.249606000	0.000001000
1	3.941395000	1.211776000	0.000000000
1	1.813140000	2.497682000	0.000000000

1a (-) _Ag^+

Atom	X	Y	Z
6	1.466898000	0.170288000	4.354798000
6	0.610787000	-0.005188000	5.432549000
6	-0.759788000	-0.194955000	5.245552000
6	-1.322109000	-0.216021000	3.978893000
6	-0.480013000	-0.042005000	2.888223000
6	0.900459000	0.148696000	3.092723000
7	1.430436000	0.287435000	1.827828000
6	0.418813000	0.184529000	0.922459000
7	-0.744404000	-0.014820000	1.536764000
16	0.599677000	0.294547000	-0.782035000
1	2.392842000	0.436392000	1.584422000
1	-2.386100000	-0.362859000	3.836182000
1	-1.396922000	-0.328208000	6.111994000
1	1.014515000	0.005711000	6.437797000
1	2.530612000	0.317507000	4.500695000
47	-1.837035000	-0.082894000	-0.555334000

2a

Atom	X	Y	Z
6	1.893296000	1.487721000	0.000000000
6	3.117000000	0.837304000	0.000000000
6	3.190841000	-0.552117000	0.000000000
6	2.038073000	-1.323402000	0.000000000
6	0.811785000	-0.680090000	0.000000000
6	0.741324000	0.716605000	0.000000000
7	-0.562502000	1.158230000	0.000000000
6	-1.544460000	0.220641000	0.000000000
16	-0.791303000	-1.357548000	0.000000000
16	-3.156616000	0.503020000	0.000000000
1	-0.825695000	2.131253000	0.000000000
1	2.094657000	-2.405012000	0.000000000
1	4.157981000	-1.039439000	0.000000000
1	4.028320000	1.422681000	0.000000000
1	1.835110000	2.569816000	0.000000000

2a (-)

Atom	X	Y	Z
6	1.872594000	1.482119000	0.000000000
6	3.104371000	0.846842000	0.000000000
6	3.194128000	-0.543638000	0.000000000
6	2.038131000	-1.316933000	0.000000000
6	0.803182000	-0.688229000	0.000000000
6	0.695212000	0.728042000	0.000000000
7	-0.563410000	1.242698000	0.000000000
6	-1.497799000	0.318078000	0.000000000
16	-0.790858000	-1.346251000	0.000000000
16	-3.167595000	0.475752000	-0.000001000
1	2.103343000	-2.399983000	0.000000000
1	4.165419000	-1.026853000	0.000000000
1	4.012454000	1.441726000	0.000000000
1	1.796272000	2.563692000	0.000000000

2a_1(-) _Ag^+

Atom	X	Y	Z
6	2.642991000	-0.031016000	-0.024848000
6	3.835459000	-0.730260000	-0.031091000
6	3.851667000	-2.125247000	-0.037226000
6	2.669810000	-2.847046000	-0.037218000
6	1.472403000	-2.147318000	-0.030982000
6	1.444549000	-0.739938000	-0.024694000
7	0.183429000	-0.196199000	-0.019227000
6	-0.758741000	-1.112571000	-0.020714000
16	-0.153947000	-2.746754000	-0.029411000
16	-2.433703000	-0.753531000	-0.014286000
1	2.682049000	-3.930287000	-0.042025000
1	4.798390000	-2.651817000	-0.042114000
1	4.772831000	-0.186523000	-0.031290000
1	2.624419000	1.052353000	-0.020144000
47	-1.522560000	1.524363000	-0.001277000

2a_2(-) _Ag^+

Atom	X	Y	Z
6	4.291339000	1.123758000	-0.154640000
6	5.434246000	0.366136000	0.018875000
6	5.361555000	-1.015758000	0.197385000
6	4.139142000	-1.666164000	0.205309000
6	2.992764000	-0.906601000	0.029380000
6	3.050101000	0.491658000	-0.151589000
7	1.838358000	1.123880000	-0.305942000
6	0.862040000	0.284764000	-0.266775000
16	1.334675000	-1.395440000	-0.035522000
16	-0.801771000	0.725634000	-0.479338000
1	4.083491000	-2.739413000	0.341148000
1	6.271104000	-1.589606000	0.329039000
1	6.402771000	0.852160000	0.014819000
1	4.336096000	2.196834000	-0.294638000
47	-1.815198000	-1.132108000	0.516729000

2a_1(-) _Ag^+_Ag(0) (Fig. 9a main text)

Atom	X	Y	Z
6	3.179062000	2.499220000	0.587630000
6	4.456522000	2.077875000	0.903957000
6	4.716046000	0.745934000	1.230671000
6	3.698393000	-0.192199000	1.247264000
6	2.416292000	0.229685000	0.928855000
6	2.143560000	1.568819000	0.597718000
7	0.823746000	1.827404000	0.307850000
6	0.081367000	0.756958000	0.401701000
16	0.940096000	-0.681995000	0.858645000
16	-1.615026000	0.793516000	0.081346000
1	3.899866000	-1.225735000	1.501807000
1	5.726309000	0.440311000	1.474705000
1	5.270706000	2.792773000	0.898429000
1	2.969977000	3.531284000	0.333570000
47	-1.068669000	3.237700000	-0.361473000
47	-2.250650000	-1.546368000	0.687371000

1a_1(-) _Ag^+_Ag(0) (Fig. 9b main text)

Atom	X	Y	Z
6	0.841415000	-1.504555000	3.250687000
6	0.105513000	-1.597473000	4.421815000
6	-1.263292000	-1.317181000	4.445170000
6	-1.944111000	-0.935854000	3.301140000
6	-1.221808000	-0.837367000	2.119017000
6	0.156045000	-1.122071000	2.110532000
7	0.552581000	-0.925797000	0.804134000
6	-0.533319000	-0.548032000	0.084226000
7	-1.616258000	-0.486890000	0.844904000
16	-0.575300000	-0.160444000	-1.598621000
1	1.472861000	-1.045455000	0.410909000
1	-3.005274000	-0.718567000	3.320052000
1	-1.802283000	-1.400504000	5.381466000
1	0.602953000	-1.892652000	5.337777000
1	1.902883000	-1.720862000	3.233956000
47	-3.030843000	0.179420000	-0.884774000
47	1.673804000	-0.969617000	-2.377501000